ELSEVIER

Journal of Hazardous Materials 141 (2007) 719–728

Journal of Hazardous Materials

www.elsevier.com/locate/jhazmat

# Preparation and evaluation of cerium(IV) tungstate powder as inorganic exchanger in sorption of cobalt and europium ions from aqueous solutions

A.M. El-Kamash *, B. El-Gammal, A.A. El-Sayed

*Hot Lab. Center, Atomic Energy Authority of Egypt, P.O. 13759, Inshas, Cairo, Egypt*

Received 24 March 2006; received in revised form 17 July 2006; accepted 18 July 2006
Available online 26 July 2006

**Abstract**

Cerium(IV) tungstate powder was chemically synthesized and exploited as adsorbent material for the decontamination study of cobalt and europium ions from radioactive waste solutions under simulated conditions using batch technique. The influences of pH, particle size and temperature have been reported. The uptake of europium was found to be slightly greater than that of cobalt and the apparent sorption capacity increases with increase in temperature. Thermodynamic parameters such as changes in Gibbs free energy ($\Delta G^\circ$), enthalpy ($\Delta H^\circ$), and entropy ($\Delta S^\circ$) were calculated. The numerical value of $\Delta G^\circ$ decreases with an increase in temperature, indicating that the sorption reaction of each ion was spontaneous and more favorable at higher temperature. The positive values of $\Delta H^\circ$ correspond to the endothermic nature of sorption processes and suggested that chemisorption was the predominant mechanism. A comparison of kinetic models applied to the sorption rate data of each ion was evaluated for the pseudo first-order, the pseudo second-order, intraparticle diffusion and homogeneous particle diffusion kinetic models. The results showed that both the pseudo second-order and the homogeneous particle diffusion models were found to best correlate the experimental rate data. The numerical values of the rate constants and particle diffusion coefficients were determined from the graphical representation of the proposed models. Activation energy ($E_a$) and entropy ($\Delta S^\ddagger$) of activation were also computed from the linearized form of Arrhenius equation.


*Keywords:* Modeling; Sorption; Kinetics; Cobalt; Europium; Cerium(IV) tungstate

## 1. Introduction

The optimization of wastewater purification processes requires a development of new operations based on low cost raw materials with high pollutant removal efficiency [1]. Research efforts have been focused on the isolation of radiocobalt and radioeuropium ions; as they constitute a significant part of radioactive liquid waste arising from nuclear facilities [2,3]. Among the methods such as chemical precipitation, oxidation, ultra-filtration, reverse osmosis and electrodialysis, ion exchange has been known for many years, particularly in the treatment of low level radioactive liquid wastes and wastewater from industrial and domestic purposes. Besides good affinity for certain ions or group of ions, the inorganic ion exchangers have been gaining popularity for ion exchange separation in waste treatment and in spent fuel reprocessing. These exchangers possess very good stability against temperature changes and high radiation levels, which make them more suitable than organic exchange resins for the treatment of radioactive liquid wastes. Recent reviews by Clearfield [4] and Lehto and Harjula [5] describe the latest developments in inorganic adsorbents and their applications in treatment of nuclear wastes. They also indicated that not many inorganic adsorbents can effectively execute the separation of fission products from acidic liquid wastes and suggested the need to develop new inorganic adsorbents that can function under these conditions.

A literature survey indicated that various synthetic inorganic adsorbents were prepared and evaluated for the removal of fission products from acidic wastes [6–18]. Also, study of sorption kinetics in wastewater treatment is important in providing valuable insights into the reaction pathways and into the mechanism of sorption reaction. Numerous theoretical models available in open literature, based on diffusion and other mechanisms, have been reported and tested by several workers using both organic and inorganic adsorbent materials [16–23]. In the present study, cerium(IV) tungstate powder was successfully prepared and

* Corresponding author. Tel.: +20 2 774 6063; fax: +20 2 462 0796.
*E-mail address:* kamash20@yahoo.com (A.M. El-Kamash).

0304-3894/$ – see front matter © 2006 Elsevier B.V. All rights reserved.
doi:10.1016/j.jhazmat.2006.07.041

used as adsorbent for the removal of cobalt and europium ions from nitrate solutions. Studies made were dedicated to the preparation process, physico-chemical characterization of prepared powder and description of sorption process. The kinetics of the sorption process has been evaluated in the light of current known models and the relevant parameters were determined.

## 2. Experimental

### 2.1. Chemicals and reagents

All the materials used in this work were of super-A pure chemicals or of equivalent analytical grade and were used without further purification. Sodium carbonate, $Na_2CO_3$ (Aldrich), tungsten trioxide, $WO_3$ (Prolabo), and cerium nitrate, $Ce(NO_3)_3{\cdot}6H_2O$ (Fisher Scientific Co., USA) were used as received. $^{60}$Co isotope was purchased from Amersham Life Science (England) while $^{152+154}$Eu was prepared by irradiating europium nitrate in the second Egyptian Research Reactor, ERR2 at the Inshas site.

### 2.2. Preparation of cerium(IV) tungstate powder

Cerium(IV) tungstate powder was chemically synthesized in a two-step procedure. Twenty grams of cerium nitrate was dissolved in a mixture of (130 mL of bidistilled water and 210 mL of isopropyl alcohol) with vigorous stirring for 2 h, followed by sol formation using 3 mL of 2 M HCl for 1 h. The sol was stabilized for 2 h and 15 mL $H_2O$ was then added in the reaction mixture. Finally, 20 mL of $NH_3$ solution was added with continuous mixing and the mixture was let stand for gelation for 4 h. The produced gel was centrifuged and dried at 50 °C for 24 h. The prepared powders were washed with bidistilled water to remove the excess ammonia and residual inorganic materials.

The resulting powder was then used in the preparation of pure cerium(IV) tungstate powder via solid-state reaction. For each sample, starting materials in the appropriate stoichiometries were thoroughly mixed so that 2 moles of sodium carbonate, 2 moles of tungsten trioxide and 1 mole of the corresponding hydrous cerium oxide are mixed and heated at 650 °C in air for 5 days with intermediate grindings. The end of the reaction and the purity of the synthesized products were confirmed by X-ray diffraction using a Shimadzu detector and Cu Kα radiation. Transparent yellow single crystals were obtained by heating the powder samples in air in platinum crucibles just above the non-congruent melting temperature, 850 °C, during 1 h and slow cooling at a rate of 5 °C/h to room temperature.

### 2.3. Characterization of cerium(IV) tungstate powder

Powder X-ray diffraction data used for least-squares refinements of lattice parameters were recorded on a Shimadzu X-ray diffractometer (XRD), model XD610 (Japan) at room temperature, using Bragg–Brentano geometry, with a back monochromatized Cu Kα radiation. Samples were very lightly ground and mounted on a flat sample plate. The diffraction pattern was scanned over the angle range 4–90 ($2\theta$) in step of 0.031 ($2\theta$) and a counting time of 10 s per step. The unit-cell parameters were refined by a least-squares procedure. Shimadzu DTA–TGA system of type DTA-TGA-50, Japan was used for the measurements of the phase changes and weight losses of the sample, respectively, at heating rate of 10 °C/min in presence of nitrogen gas to avoid thermal oxidation of the powder sample. The morphology of the prepared cerium tungstate powders was studied using scanning electron microscopy. Samples were washed, dried and mounting on support and then made conductive with sputtered gold. The surface observations were made using JEOL JSM-5400 Scanning Electron Microscope. For each case, the presence of the metal elements Na, Ce and W in the prepared crystals was confirmed by energy dispersive spectroscopy analysis (EDX) connected to the Scanning Electron Microscope system.

### 2.4. Kinetic measurements

Batch experiments with 100 μm cerium(IV) tungstate particles and $10^{-4}$ M initial metal ion concentration were conducted to investigate the parametric effects of the initial adsorbate pH on the sorption process. Cobalt and europium samples were prepared by dissolving a known quantity of both cobalt(II) nitrate and europium(III) nitrate, respectively, in double-distilled water and used as a stock solution, which was labelled with $^{60}$Co and $^{152+154}$Eu radioisotopes. The pH of each solution was adjusted with liquid ammonia solution (35%) and 1 M HCl solution.

The kinetic behavior of $Co^{2+}$ and $Eu^{3+}$ ions on cerium(IV) tungstate powder was also followed up by application of batch technique. 0.25 g of the prepared powder was shaken at 298, 303, 318, and 333 K with 50 mL of $5 \times 10^{-3}$ M for each ion at a speed of 250 rpm in a thermostatic shaker for a specified period of contact time. Then, a fixed volume (2 mL) of the aliquot was withdrawn as a function of time while the solution was being continuously shaken. Thus, the ratio of the volume of the solution to the weight of the adsorbent in the flask does not change from the original ratio. To avoid colloidal suspension in the solutions to be analyzed, the withdrawn solution was highly centrifuged using 5500 rpm, MLW Zentrifugenban Co. (Germany), for 3 min. A fixed volume (1 mL) of the clear solution was pipetted out for the determination of the amount of unsorbed metal ion. The concentration of the metal ion in solution was determined radiometrically, using NaI(Tl) scintillation detector connected to an ORTEC assembly (Nuclear Enterprises), USA. The amount of metal ion sorbed onto cerium(IV) tungstate phase at any time, $q_t$ (mmol/g) and the percentage adsorption ($P$) were calculated from the expressions:

$$q_t = \left(\frac{A_0 - A_t}{A_0}\right) C_0 \frac{V}{m} \quad (1)$$

$$P = \left(\frac{A_0 - A_t}{A_0}\right) \times 100 \quad (2)$$

where $A_0$ and $A_t$ are the initial and time interval activities of metal ion in solution, $V$ the volume (L), $m$ the weight (g) of the adsorbent, and $C_0$ is the initial concentration (mmol/L) of the metal ion used. The sorption process was continued for sufficient long time (∼24 h), and the distribution coefficient, $K_d$ was

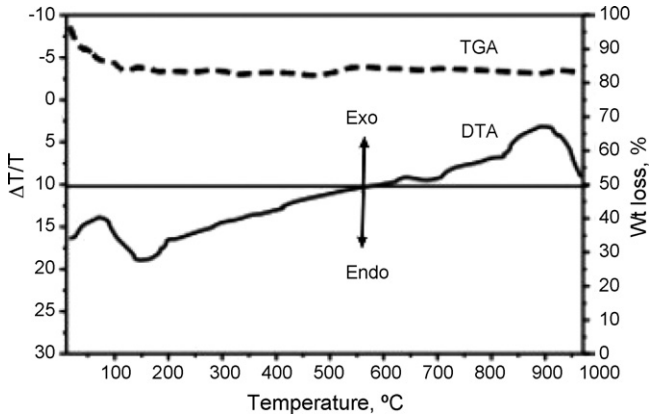


Fig. 1. DTA–TGA thermogram of cerium(IV) tungstate prepared by the solid-state reaction.

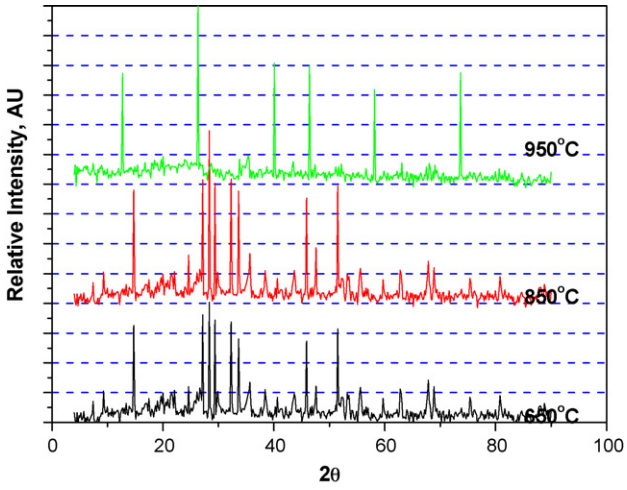


Fig. 2. X-ray diffraction patterns of cerium(IV) tungstate fired at different temperatures.

calculated from the equation:

$$K_d = \left[\frac{A_0 - A_e}{A_e}\right]\frac{V}{m} \times 10^3 \quad (3)$$

where $A_e$ is the radioactivity of the solution after equilibrium.

All the experiments were carried out in duplicate and the mean values are presented.

## 3. Results and discussion

### 3.1. Characterization of cerium(IV) tungstate powder

Fig. 1 shows the simultaneous DTA–TGA analysis of cerium(IV) tungstate powder prepared by the solid-state reaction at 650 °C. The TGA curve indicates a weight loss of the sample starting at about 90 °C of about 12 wt%, which is attributed to the removal of physically adsorbed water as confirmed by the endothermic peak of the DTA curve at the same temperature. An exothermic peak began to appear above 850 °C, which may be assigned to a phase transformation of $Na_3{\cdot}Ce(WO_3)_2O_8$ to form $Na_{10}{\cdot}Ce_8(W_5O_{20})O_8$ at this temperature without any formation of decomposition products.

Fig. 2 shows the X-ray diffraction patterns of cerium(IV) tungstate powder after firing at different temperatures. The XRD data showed that the prepared raw material at 650 °C is mainly composed of cerium tungstate in its sodium form as $Na_3{\cdot}Ce(WO_3)_2O_8$. This temperature was at least 185–200 °C lower than that of the cerium(IV) tungstate formed as a result of the reaction between sodium carbonate, tungsten trioxide and cerium oxide through their solid-state reaction at 850 °C. The structure of the prepared cerium tungstate remained constant on raising the firing temperature to 850 °C except for the crystallinity of the compound was enhanced. When the powder samples are heated widely above the melting point, typically 100 °C above, the results, according to [24], were a mixture of two types of single crystals, yellow crystals of $Na_3{\cdot}Ce(WO_3)_2O_8$ and orange colored single crystals corresponding to compounds $Na_{10}{\cdot}Ce_8(W_5O_{20})O_8$.

These results were qualitatively verified using complimentary EDX sensor connected the SEM unit. The topography of the prepared cerium tungstate products was monitored using SEM and viewed in Fig. 3. The surface structure of $Na_3{\cdot}Ce(WO_3)_2O_8$ is more rough than $Na_{10}{\cdot}Ce_8(W_5O_{20})O_8$. However, the structure of both compounds contains a network of interconnected pore streams that lie in the micrometer range.

### 3.2. Kinetic studies

#### 3.2.1. Effect of pH

To determine the chemical condition at which $Co^{2+}$ and $Eu^{3+}$ ions are effectively sorbed onto prepared cerium(IV) tungstate

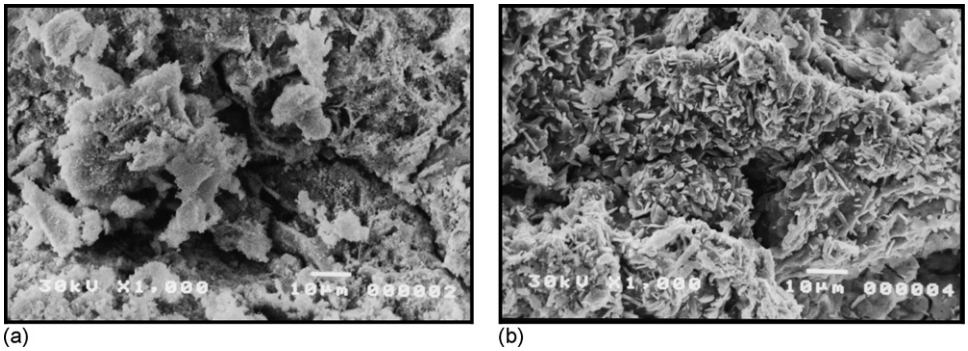


Fig. 3. Scanning electron micrographs of cerium(IV) tungstate (a) $Na_3{\cdot}Ce(WO_3)_2O_8$ and (b) $Na_{10}{\cdot}Ce_8(W_5O_{20})O_8$.

powder, the sorption was studied at different pH ranging from 3.0 to 8.0. It was observed that the uptake of each ion was inhibited in the acidic medium, pH < 2.0. This could be attributed to the competition between hydrogen ion and studied ions for sorption onto prepared powder. The highest uptake was observed for $Eu^{3+}$ at pH range 3.0–4.0. At higher pH values, the uptake of $Eu^{3+}$ ions was slightly decreased, which may be attributed to the variation of the chemical species, due to the formation of the hydroxide complexes of $Eu^{3+}$ ions in solution [25]. The uptake of $Co^{2+}$ ions increased with pH particularly in pH range 4.0–8.0. All future sorption studies were carried out at pH 6.0 and pH 4.0 for $Co^{2+}$ and $Eu^{3+}$ ions, respectively.

### 3.2.2. *Effect of particle size*

Fig. 4 shows plots of the amount sorbed of $Co^{2+}$ and $Eu^{3+}$ ions from nitrate solutions for various adsorbent particle sizes. The adsorbent diameters shown are the averages of the mesh sizes for the consecutive sieves that allowed the particles to pass through and retained the particles. It is clear from the figure that the metal ion removal rate significantly affected by the particle size. The rate and extent of sorption, for a constant mass of the adsorbent, is proportional to the specific surface area, which is higher for small particles. Guibal et al. [26] reported that mathematical models for external surface diffusion and intraparticle diffusion-controlled sorption dictated that the sorption rate parameters should vary with the reciprocal of the first power of the adsorbent particle diameter and the reciprocal of some power of the adsorbent particle diameter, respectively. On the other hand, if the interaction between the sorbate and the binding sites is kinetically rate controlled, the rate constant, and hence sorption rate, will be independent of the adsorbent particle size [27].

### 3.2.3. *Effect of contact time and temperature*

Fig. 5 shows plots of the amount sorbed of $Co^{2+}$ and $Eu^{3+}$ ions from aqueous nitrate solutions onto prepared cerium(IV) tungstate powder, at initial metal ion concentration of $5 \times 10^{-3}$ M and at temperature range of 298–333 K, as a function of contact time. The figure shows a high initial rate of removal within the first 2 h of contact (over 80% removed) followed by a slower subsequent removal rate that gradually approached an equilibrium conditions in 5 h. The metal ions fraction sorbed and their corresponding distribution coefficient values were calculated at different temperatures using Eqs. (2) and (3) and summarized in Table 1. It is evident that these parameters were dependent on temperature and their values increased with increasing temperature indicating the endothermic nature of the sorption processes of both studied ions. In order to gain

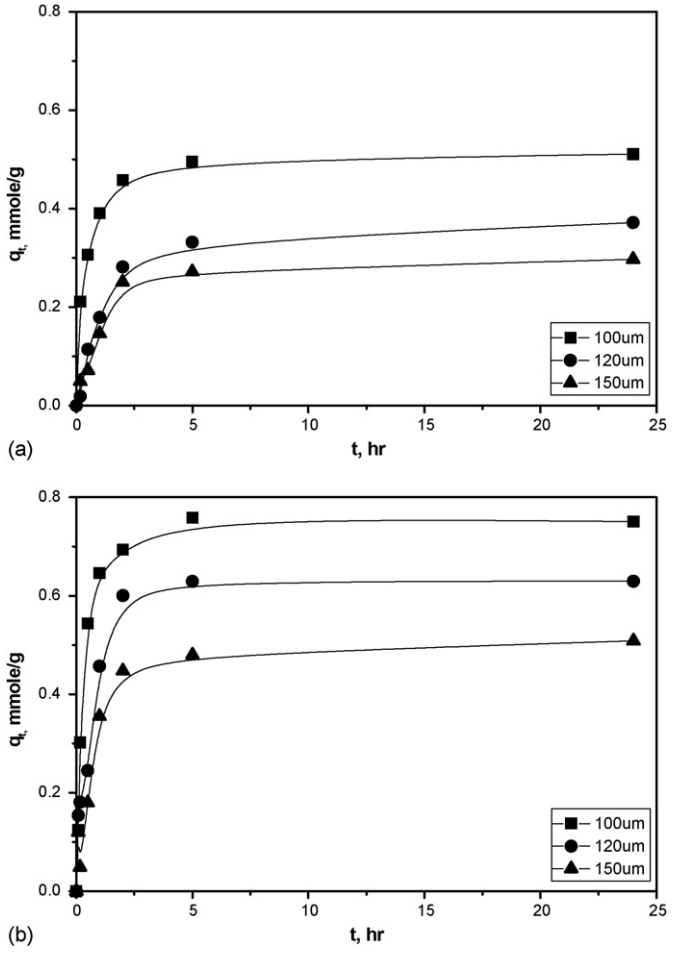


Fig. 4. Plots of the amount sorbed of (a) $Co^{2+}$ and (b) $Eu^{3+}$ ions from aqueous nitrate solutions onto different particle sizes of cerium(IV) tungstate powder.

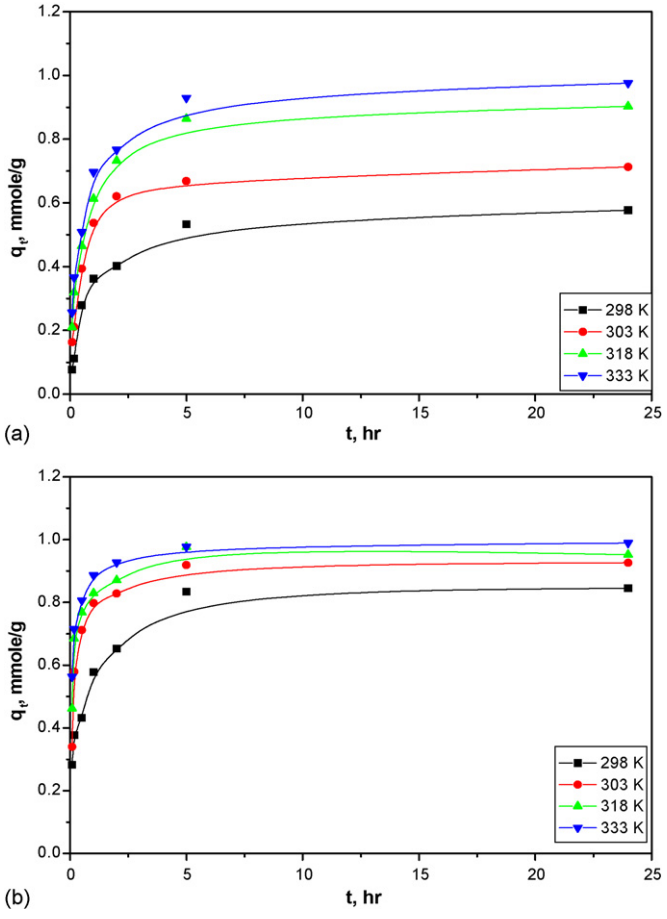


Fig. 5. Effect of contact time on the amount sorbed of (a) $Co^{2+}$ and (b) $Eu^{3+}$ from aqueous nitrate solutions onto cerium(IV) tungstate powder at different temperatures.

Table 1
Equilibrium characteristics and thermodynamic parameters for the sorption of $Co^{2+}$ and $Eu^{3+}$ ions on cerium(IV) tungstate at different reaction temperatures

| Temperature (K) | $P$ (%) | | $K_d$ (mL/g) | | $K_c = F_e/(1-F_e)$ | | $\Delta G^\circ$ (kJ/mol) | | $\Delta H^\circ$ (kJ/mol) | | $\Delta S^\circ$ (J/mol K) | |
|---|---|---|---|---|---|---|---|---|---|---|---|---|
| | $Co^{2+}$ | $Eu^{3+}$ | $Co^{2+}$ | $Eu^{3+}$ | $Co^{2+}$ | $Eu^{3+}$ | $Co^{2+}$ | $Eu^{3+}$ | $Co^{2+}$ | $Eu^{3+}$ | $Co^{2+}$ | $Eu^{3+}$ |
| 298 | 56.0 | 85.0 | 250 | 1130 | 1.27 | 5.67 | −0.59 | −4.30 | | | | |
| 303 | 70.0 | 93.0 | 470 | 2650 | 2.33 | 13.28 | −2.13 | −6.52 | 85.19 | 61.63 | 287.85 | 222.40 |
| 318 | 91.0 | 96.0 | 2020 | 4800 | 10.11 | 24.00 | −6.12 | −8.40 | | | | |
| 333 | 98.0 | 99.0 | 9800 | 19800 | 49.00 | 99.00 | −10.78 | −12.72 | | | | |

insight into the thermodynamic nature of the sorption process, several thermodynamic parameters for the present systems were calculated. The Gibbs free energy change, $\Delta G^\circ$, is the fundamental criterion of spontaneity. Reactions occur spontaneously at a given temperature if $\Delta G^\circ$ is a negative quantity. The free energy of the sorption reaction is given by the following equation:

$$\Delta G^\circ = -RT \ln K_c \quad (4)$$

where $K_c$ is the sorption equilibrium constant, $R$ the gas constant, and $T$ is the absolute temperature (K). The sorption equilibrium constant ($K_c$) can calculated from:

$$K_c = \frac{F_e}{1 - F_e} \quad (5)$$

where $F_e$ is the fraction attainment of metal ion sorbed at equilibrium.

The values of the equilibrium constant ($K_c$) for the sorption of $Co^{2+}$ and $Eu^{3+}$ ions onto cerium(IV) tungstate powder were calculated at different temperatures and at equilibrium time of 24 h using Eq. (5). The variation of $K_c$ with temperature, as summarized in Table 1, showed that $K_c$ values increase with increase in sorption temperature, thus implying a strengthening of adsorbate–adsorbent interactions at higher temperature. This also indicates that $Co^{2+}$ and/or $Eu^{3+}$ ions dehydrate considerably at higher temperature before sorption and thus their sizes during sorption are smaller yielding higher $K_c$ values [28]. Also, the obtained negative values of $\Delta G^\circ$ confirm the feasibility of the process and the spontaneous nature of the sorption processes with preference towards $Eu^{3+}$ than $Co^{2+}$ ions.

The Gibbs free change can be represented as follows:

$$\Delta G^\circ = \Delta H^\circ - T\,\Delta S^\circ \quad (6)$$

The values of enthalpy change ($\Delta H^\circ$) and entropy change ($\Delta S^\circ$) calculated from the slope and intercept of the plot of $\Delta G^\circ$ versus $T$ (Fig. 6) are also given in Table 1. The change in $\Delta H^\circ$ for both ions was found to be positive confirming the endothermic nature of the sorption process. It is of note that $\Delta H^\circ$ due to chemisorption takes values between 40 and 120 kJ/mol [29]. Therefore, chemisorption is the predominant mechanism for the sorption of the examined ions. The positive values of the entropy change ($\Delta S^\circ$) show the increased randomness at the solid/solution interface with some structural changes in the adsorbate and adsorbent and an affinity of the cerium(IV) tungstate powder towards $Co^{2+}$ and/or $Eu^{3+}$ ions.

### 3.3. Sorption kinetics modeling

The study of sorption dynamics describes the solute uptake rate and evidently this rate controls the residence time of adsorbate uptake at the solid/solution interface. In this part of study, the data of the kinetics of $Co^{2+}$ and $Eu^{3+}$ ions sorbed from aqueous nitrate solutions onto prepared cerium(IV) tungstate powder, as illustrated in Fig. 5, were analyzed using pseudo first-order, pseudo second-order, intraparticle diffusion and homogeneous particle diffusion kinetic models, respectively. The conformity between experimental data and each model predicted values was expressed by the correlation coefficient ($R^2$). A relatively high $R^2$ values indicates that the model successfully describes the kinetics of metal ion sorption removal.

#### 3.3.1. Pseudo first-order model

The sorption kinetics of metal ions from liquid phase to solid is considered as a reversible reaction with an equilibrium state being established between two phases. A simple pseudo first-order model [27–30] was therefore used to correlate the rate of reaction and expressed as follows:

$$\frac{dq_t}{dt} = k_1(q_e - q_t) \quad (7)$$

where $q_e$ and $q_t$ are the concentrations of ion in the adsorbent at equilibrium and at time $t$, respectively (mmol/g) and $k_1$ is the pseudo first-order rate constant ($h^{-1}$).

After integration and applying boundary conditions $t = 0$ to $t = t$ and $q_t = 0$ to $q_t = q_t$, the integrated form of Eq. (7) becomes:

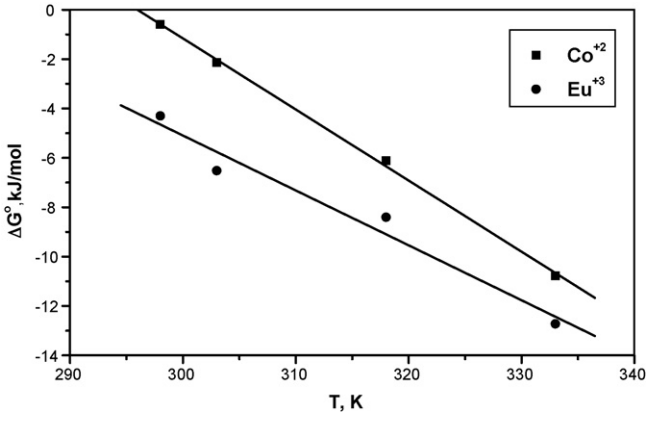


Fig. 6. Relationship between Gibbs free energy change and temperature of sorption of $Co^{2+}$ and $Eu^{3+}$ ions onto cerium(IV) tungstate powder.

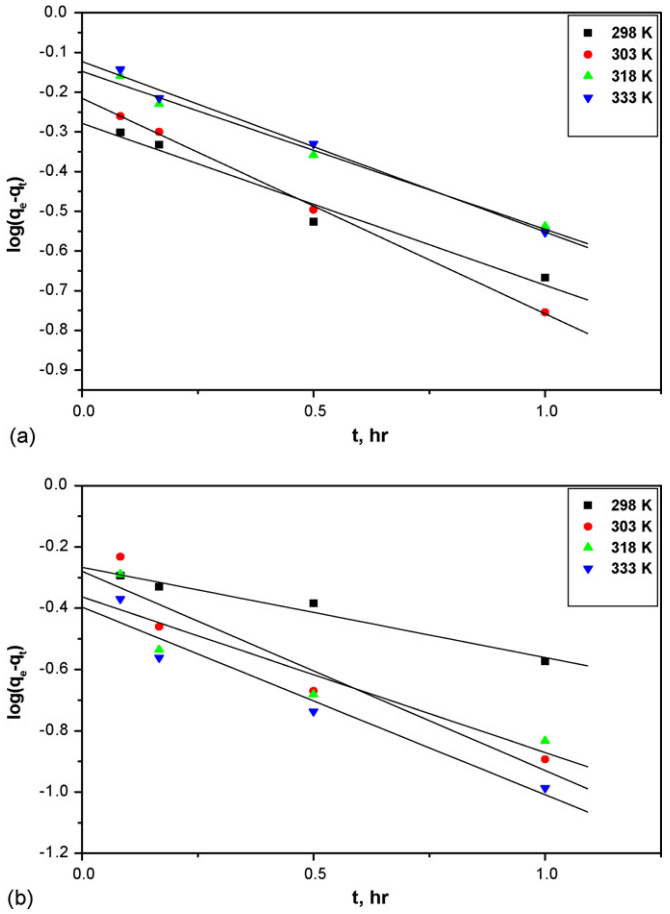


Fig. 7. Pseudo first-order kinetic plots for the sorption of (a) $Co^{2+}$ and (b) $Eu^{3+}$ from aqueous solutions onto cerium(IV) tungstate powder.

$$\log(q_e - q_t) = \log q_e - \frac{k_1}{2.303}t \tag{8}$$

Plots for Eq. (8) were made for $Co^{2+}$ and $Eu^{3+}$ ions sorption at different studied temperatures, and shown in Fig. 7. Approximately linear fits were observed for the two ions, over the entire range of shaking time explored and at all temperatures, with low correlation coefficients, indicating that the pseudo first-order kinetic model is not valid for the present systems.

### 3.3.2. Pseudo second-order model

A pseudo second-order rate model [30,31] is also used to describe the kinetics of the sorption of ions onto adsorbent materials. The differential equation for chemisorption kinetic rate reaction is expressed as:

$$\frac{dq_t}{dt} = k_2(q_e - q_t)^2 \tag{9}$$

where $k_2$ is the rate constant of pseudo second-order equation (g/mmol h).

For the boundary conditions $t = 0$ to $t = t$ and $q_t = 0$ to $q_t = q_t$, the integrated form of Eq. (9) becomes:

$$\frac{1}{q_e - q_t} = \frac{1}{q_e} + k_2 t \tag{10}$$

Eq. (10) can be rearranged to obtain a linear form equation as:

$$\left(\frac{t}{q_t}\right) = \left(\frac{1}{k_2 q_e^2}\right) + \left(\frac{1}{q_e}\right)t \tag{11}$$

If the initial sorption rate $h$ (mmol/g h) is:

$$h = k_2 q_e^2 \tag{12}$$

Then Eqs. (11) and (12) becomes:

$$\frac{t}{q_t} = \frac{1}{h} + \frac{1}{q_e}t \tag{13}$$

The kinetic plots of $t/q_t$ versus $t$ for $Co^{2+}$ and $Eu^{3+}$ ions sorption at different temperatures are presented in Fig. 8. The relationships are linear, and the values of the correlation coefficient ($R^2$), suggest a strong relationship between the parameters and also explain that the process of sorption of each ion follows pseudo second-order kinetic model. From Table 2, it can be shown that the values of the initial sorption rate '$h$' and rate constant '$k_2$' were increased with increase in temperature. The correlation coefficient $R^2$ has an extremely high value (>0.99), and the theoretical $q_e$ values agree with the experimental ones. These results suggest that the pseudo second-order sorption mechanism is pre-

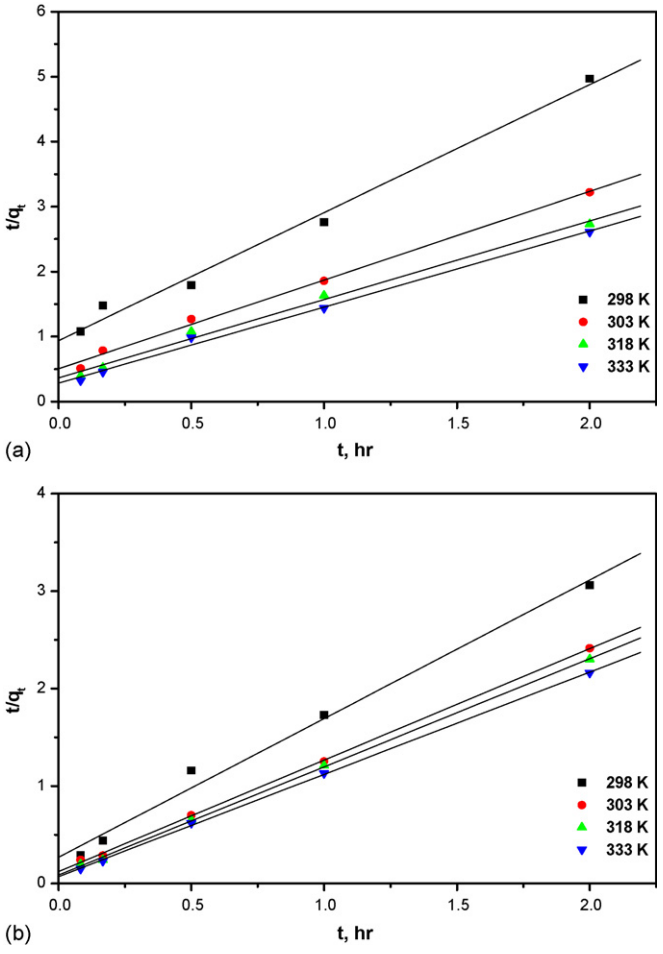


Fig. 8. Pseudo second-order kinetic plots for the sorption of (a) $Co^{2+}$ and (b) $Eu^{3+}$ from aqueous solutions onto cerium(IV) tungstate powder.

Table 2
The calculated parameters of the pseudo second-order kinetic models for $Co^{2+}$ and $Eu^{3+}$ ions sorbed onto cerium(IV) tungstate

| Temperature (K) | $q_e$ (mmol/g) | | $h$ (mmol/g h) | | $k_2$ (g/mmol h) | | $R^2$ | |
|---|---|---|---|---|---|---|---|---|
| | $Co^{2+}$ | $Eu^{3+}$ | $Co^{2+}$ | $Eu^{3+}$ | $Co^{2+}$ | $Eu^{3+}$ | $Co^{2+}$ | $Eu^{3+}$ |
| 298 | 0.507 | 0.703 | 1.066 | 3.719 | 4.147 | 7.528 | 0.9951 | 0.9940 |
| 303 | 0.733 | 0.874 | 1.976 | 8.146 | 3.679 | 10.640 | 0.9976 | 0.9990 |
| 318 | 0.828 | 0.901 | 2.743 | 11.494 | 3.996 | 14.158 | 0.9966 | 0.9997 |
| 333 | 0.854 | 0.953 | 3.520 | 14.033 | 4.829 | 15.440 | 0.9974 | 0.9998 |

dominant and that the over all rate constant of each ion appears to be controlled by the chemisorption process.

### 3.3.3. Intraparticle diffusion model

The intraparticle diffusion model, Morris and Weber model [32], is expressed as:

$$q_t = K_{ad}\, t^{1/2} \tag{14}$$

where $K_{ad}$ is the rate constant of intraparticle transport (mmol/g $h^{1/2}$).

According to this model, plotting a graphic of $q_t$ versus $t^{1/2}$, if a straight line passing through the origin is obtained, it can be assumed that the involved mechanism is a diffusion of the species. In this case the slope of the linear plot is the rate constant of intraparticle transport. As can be seen in Fig. 9, for times up to 1 h, the Morris–Weber relationship holds good at all studied temperatures and the values of $K_{ad}$ were calculated, from the slope of the linear plots obtained, and presented in Table 3.

### 3.3.4. Homogeneous particle diffusion model (HPDM)

In this model, the rate-determining step of sorption is normally described by either (a) diffusion of ions through the liquid film surrounding the particle, called film diffusion, or (b) diffusion of ions into the sorbent beads, called particle diffusion mechanism. Nernst–Plank equation [33], which takes into account both concentration and electrical gradients of exchanging ions into the flux equation, was used to establish the HPDM equations. If the diffusion of ions from the solution to the sorbent beads is the slowest step, rate-determining step, the liquid film diffusion model controls the rate of sorption. In such case, the following relation can be utilized to calculate the diffusion coefficient:

$$-\ln(1-X) = \frac{3DC}{r_0 \delta C_r} t \tag{15}$$

Table 3
Intraparticle diffusion rate constant for the sorption of $Co^{2+}$ and $Eu^{3+}$ ions onto cerium tungstate

| Temperature (K) | $K_{ad}$ (mmol/g $h^{1/2}$) | | $R^2$ | |
|---|---|---|---|---|
| | $Co^{2+}$ | $Eu^{3+}$ | $Co^{2+}$ | $Eu^{3+}$ |
| 298 | 0.515 | 0.629 | 0.985 | 0.953 |
| 303 | 0.570 | 0.846 | 0.952 | 0.973 |
| 318 | 0.728 | 0.880 | 0.979 | 0.959 |
| 333 | 0.760 | 0.974 | 0.999 | 0.955 |

where $C$ and $C_r$ are the equilibrium concentrations of the ion in solution and solid phases, respectively, $D$ the diffusion coefficient in the liquid phase, $X$ the fraction attainment of equilibrium or extent of adsorbent conversion, $r_0$ the radius of the adsorbent particle, and $\delta$ is the thickness of the liquid film.

If the diffusion of ions through the adsorbent beads is the slowest step, the particle diffusion will be the rate-determining step and the particle diffusion model could apply to calculate the diffusion coefficients. Then, the rate equation is expressed by:

$$-\ln(1-X^2) = \frac{2D_r\pi^2}{r_0^2} t \tag{16}$$

where $D_r$ is the particle diffusion coefficient.

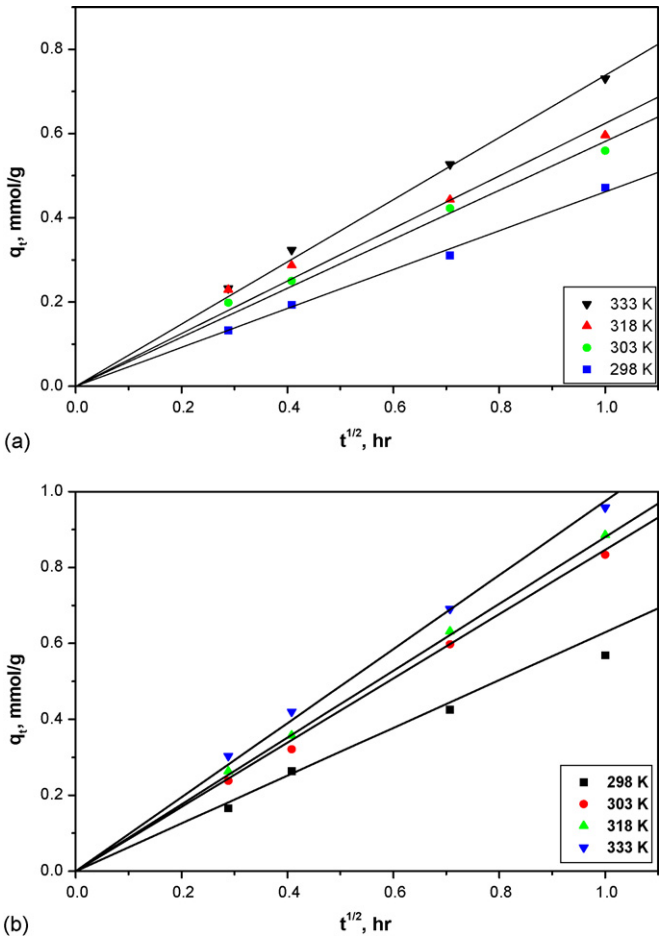


Fig. 9. Morris–Weber kinetic plots for the sorption of (a) $Co^{2+}$ and (b) $Eu^{3+}$ from aqueous solutions onto cerium(IV) tungstate powder.

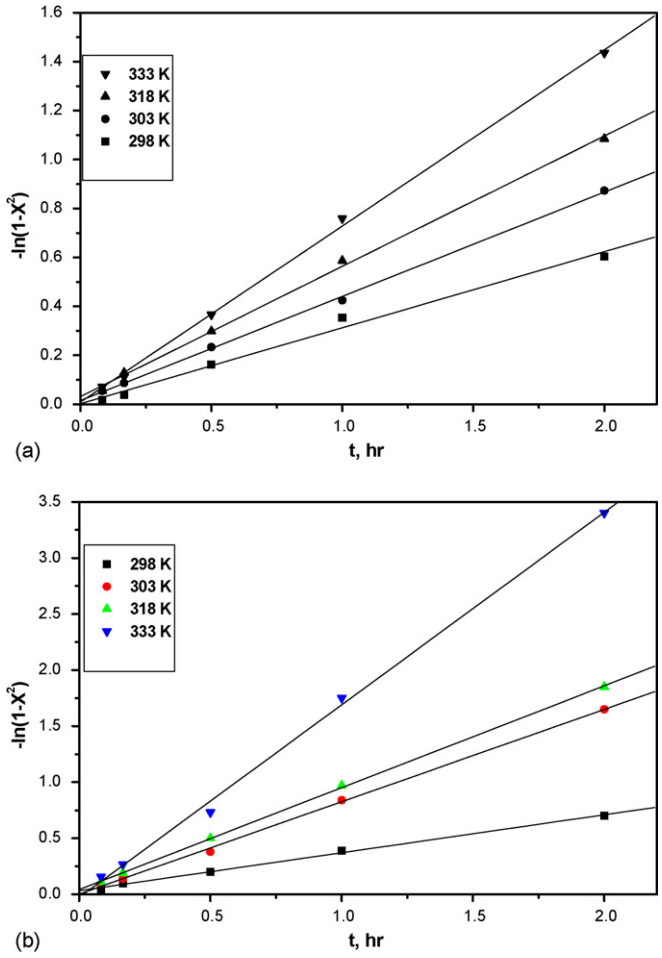


Fig. 10. Plots of $-\ln(1-X^2)$ as a function of time for the diffusion of (a) $Co^{2+}$ and (b) $Eu^{3+}$ from aqueous solutions onto cerium(IV) tungstate powder.

The two previous model equations (Eqs. (15) and (16)) were tested against the kinetic rate data of both $Co^{2+}$ and $Eu^{3+}$ ions sorbed onto cerium(IV) tungstate powder by plotting the functions of $-\ln(1-X)$ and $-\ln(1-X^2)$ against contact time. The straight lines that are obtained in the case of $-\ln(1-X)$ versus time does not pass through the origin (graphs omitted), indicating that the film diffusion model does not controls the rate of the sorption processes. On the other hand, the straight lines of the plots of $-\ln(1-X^2)$ versus contact time, as shown in Fig. 10, pass through the origin for both ions indicating that the particle diffusion model controls the sorption processes at all studied temperatures. The slope values of these plots were used to calculate the effective diffusion coefficients ($D_r$) using Eq. (16). These calculated values together with the correlation coefficient ($R^2$) for both ions are presented in Table 4. The magnitude of the diffusion coefficient is dependent upon the nature of the sorption process. For physical adsorption, the value of the effective diffusion coefficient ranges from $10^{-6}$ to $10^{-9}$ $m^2/s$ and for chemisorption, the value ranges from $10^{-9}$ to $10^{-17}$ $m^2/s$ [34]. The difference in the values is due to the fact that in physical adsorption the molecules are weakly bound and therefore there is ease of migration, whereas for chemisorption the molecules are strongly bound and mostly localized. Therefore, from this

Table 4
Diffusion coefficients for the sorption of $Co^{2+}$ and $Eu^{3+}$ ions onto cerium(IV) tungstate

| Temperature (K) | $D_r \times 10^{14}$ ($m^2/s$) | | $R^2$ | |
|---|---|---|---|---|
| | $Co^{2+}$ | $Eu^{3+}$ | $Co^{2+}$ | $Eu^{3+}$ |
| 298 | 4.37 | 4.76 | 0.995 | 0.993 |
| 303 | 5.99 | 11.58 | 0.992 | 0.993 |
| 318 | 7.49 | 12.78 | 0.999 | 0.999 |
| 333 | 10.12 | 24.16 | 0.999 | 0.995 |

research, the most likely nature of sorption is chemisorption since the values of $D_r$ were in the order $10^{-14}$ $m^2/s$ for both ions. This is in agreement with the pseudo second-order kinetic model. Also, based on the values of the correlation coefficient ($R^2$) obtained for all tested models, the pseudo second-order and PHDM models were found to best correlate the rate kinetic data of the sorption of both ions.

On the other hand, plotting of $\ln D_r$ versus $1/T$ gave a straight line, as shown in Fig. 11, proves the validation of the linear form of Arrhenius equation:

$$\ln D_r = \ln D_0 - \left(\frac{E_a}{RT}\right) \quad (17)$$

where $D_0$ is a pre-exponential constant analogous to Arrhenius frequency factor.

The energies of activation for both ions, $E_a$, were calculated from the slope of the straight lines in Fig. 11 and the obtained values were presented in Table 5. Values of $E_a$ below 42 kJ/mol generally indicate diffusion-control processes and higher values represent chemical reaction processes [35]. Such a low value of

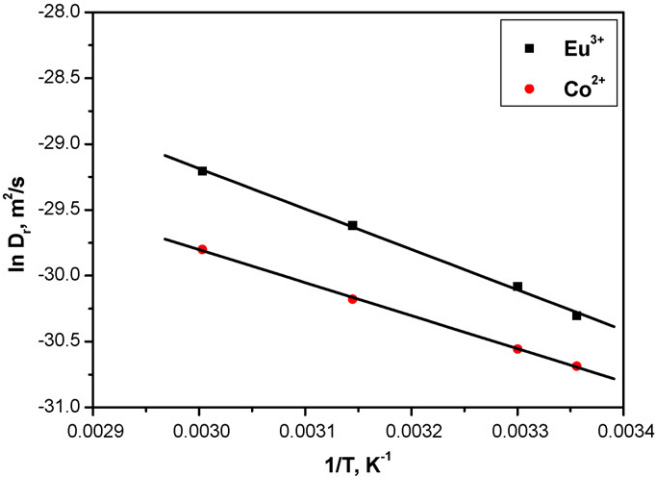


Fig. 11. Arrhenius plots for the particle diffusion coefficients of $Co^{2+}$ and $Eu^{3+}$ ions sorbed onto cerium(IV) tungstate powder.

Table 5
Kinetic parameters for the sorption of $Co^{2+}$ and $Eu^{3+}$ ions onto cerium(IV) tungstate

| Metal ion | $D_0$ ($m^2/s$) | $E_a$ (kJ/mol) | $\Delta S^{\ddagger}$ (J/mol K) |
|---|---|---|---|
| $Co^{2+}$ | $0.21 \times 10^{-9}$ | 20.85 | −158.95 |
| $Eu^{3+}$ | $2.11 \times 10^{-9}$ | 25.52 | −139.77 |

the activation energy for the sorption of each metal ion indicates a chemical sorption process involving weak interaction between adsorbent, cerium(IV) tungstate, and sorbate ($Co^{2+}$ and/or $Eu^{3+}$) and suggests that each sorption process has a low potential energy. The Arrhenius equation would be also used to calculate $D_0$, which in turn is used for the calculation of entropy of activation ($\Delta S^{\ddagger}$) of the sorption process using [36]:

$$D_0 = \left(\frac{2.72d^2KT}{h}\right) \exp\left(\frac{\Delta S^{\ddagger}}{R}\right) \quad (18)$$

where $K$ is the Boltzmann constant, $h$ the Plank constant, $d$ the distance between two adjacent active sites in the solid matrix, $R$ the gas constant, and $T$ is the absolute temperature. Assuming that the value of $d$ is equal to $5 \times 10^{-8}$ cm [36], the values of $\Delta S^{\ddagger}$ for both ions were calculated and presented in Table 5. The value of entropy of activation ($\Delta S^{\ddagger}$) is an indication of whether or not the reaction is an associative or dissociative mechanism. $\Delta S^{\ddagger}$ values $> -10$ J/mol K generally imply a dissociative mechanism [35]. However, the high negative values of $\Delta S^{\ddagger}$ obtained in this study (Table 5) suggested that each $Co^{2+}$ or $Eu^{3+}$ ions sorption on cerium(IV) tungstate powder is an associative mechanism.

## 4. Conclusion

Cerium(IV) tungstate powder was chemically prepared, characterized using DTA–TGA, XRD, and SEM measurements and tested as adsorbent material for the removal of cobalt and europium ions from nitrate solutions. The kinetics of these ions was experimentally studied and the obtained rate data were analyzed using the pseudo first-order, the pseudo second-order, intraparticle diffusion and homogeneous particle diffusion kinetic models. Based on the values of the correlation coefficient ($R^2$) obtained for all tested models, both pseudo second-order and PHDM models were found to best correlate the rate kinetic data of both ions. The magnitudes of the particle diffusion coefficients of both ions were in the order of $10^{-14}$ $m^2/s$ indicating a chemisorption nature for the sorption processes. The values of $E_a$ obtained are $< 42$ kJ/mol, indicating a diffusion-controlled process and based on $\Delta S^{\ddagger}$ values, the sorption reaction of each studied ion is an associative mechanism.

## References


[1] J. Peric, M. trgo, N.V. Medvidovic, Removal of zinc, copper and lead by natural zeolite—a comparison of adsorption isotherms, Water Res. 38 (2004) 1839–1899.

[2] A.A. Helal, H.F. Aly, S.M. Khalifa, M.I. Ahmed, Sorption of radiocobalt on pottery, Radiochim. Acta 93 (2005) 471–476.

[3] A.A. Helal, M.I. Ahmed, S.M. Khalifa, H.F. Aly, Decontamination of radioactive waste solution by using pottery, Radiochemistry 48 (4) (2006) 321–328.

[4] A. Clearfield, Inorganic ion exchanger past present and future, Solvent Extr. Ion Exch. 18 (2000) 655–678.

[5] J. Lehto, R. Harjula, Selective separation of radionuclides from nuclear waste solutions with inorganic ion exchangers, Radiochim. Acta 86 (1999) 65–70.

[6] M.V. Sivaah, K.A. Venkatesan, R.M. Krishna, P. Sasidhar, G.S. Murthy, Ion exchange studies of europium on uranium antimonate, Colloid Surf. A 236 (2004) 147–157.

[7] E.S. Zakaria, I.M. Ali, I.M. El-Naggar, Thermodynamics and ion exchange equilibria of $Gd^{3+}$, $Eu^{3+}$ and $Ce^{3+}$ ions on $H^+$ form of titanium(IV) antimonate, Colloid Surf. A 210 (2002) 33–40.

[8] T.J. Tranter, R.S. Herbst, T.A. Todd, A.L. Olson, H.B. Eldredge, Evaluation of ammonium molybdophosphate-polyacrylonitrile (AMP-PAN) as a cesium selective sorbent for the removal of $^{137}Cs$ from acidic nuclear waste solutions, Adv. Environ. Res. 6 (2002) 107–121.

[9] F. Sebesta, Methods for modification of properties of inorganic ion-exchangers for application in column beds, J. Radioanal. Nucl. Chem. 220 (1997) 77–88.

[10] S.A. Stout, Y. Cho, S. Komarneni, Uptake of cesium and strontium cations by potassium-depleted phlogopite, Appl. Clay Sci. 31 (2006) 306–313.

[11] A. Nilchi, B. Maalek, A. Khanchi, M.G. Margheh, A. Bagheri, Cerium(IV) molybdate cation exchanger: synthesis, properties and ion separation capabilities, Radiat. Phys. Chem. 75 (2006) 301–308.

[12] Y.S. Dzyazko, L.M. Rozhdesvenska, A.V. Palchik, F. Lapicque, Ion exchange properties and mobility of $Cu^{2+}$ ion in zirconium hydro phosphate ion exchangers, Sep. Purif. Technol. 45 (2005) 141–146.

[13] V.S. Bergamaschi, F.M.S. Carvalho, C. Rodrigues, V.B. Fernandes, Preparation and evaluation of zirconia microspheres as inorganic exchanger in adsorption of copper and nickel ions and as catalyst in hydrogen production from bioethanol, Chem. Eng. J. 112 (2005) 153–158.

[14] K.M. Abd El-Rahman, A.M. El-Kamash, M.R. El-Sourougy, N.M. ABdel-Moniem, Thermodynamic modeling for the removal of $Cs^+$, $Sr^{2+}$, $Ca^{2+}$, and $Mg^{2+}$ ions from aqueous waste solutions using zeolite A, J. Radioanal. Nucl. Chem. 288 (2006) 221–230.

[15] H.H. Someda, A.A. El Zahhar, M.K. Shehata, H.A. El-Naggar, Supporting of some ferrocyanides on polyacrylonitrile (PAN) binding polymer and their application for cesium treatment, Sep. Purif. Technol. 29 (2002) 53–61.

[16] A.M. El-Kamash, A.A. Zaki, M. Abd El Geleel, Modeling batch kinetics and thermodynamics of zinc and cadmium ions removal from waste solutions using synthetic zeolite A, J. Hazard Mater. 127 (2005) 211–220.

[17] M.M. Abou-Mesalam, I.M. El-Naggar, Diffusion mechanism of $Cs^+$, $Zn^{2+}$ and $Eu^{3+}$ ions in the particles of zirconium titanate ion exchanger using radioactive tracers, Colloid Surf. A 215 (2003) 205–211.

[18] I.M. Ismail, M. Nogami, K. Suzuki, Effect of pore diameter of TMMA chelating resin beads on the adsorption properties of U(VI) and Ce(III) from different media, Sep. Purif. Technol. 31 (2003) 231–239.

[19] M.S. Onyango, H. Matsuda, T. Ogada, Sorption kinetics of arsenic onto iron conditioned zeolite, J. Chem. Eng. Japan 36 (2003) 477–485.

[20] M.S. Onyango, Y. Kojima, H. Matsuda, A. Ochieng, Adsorption kinetics of arsenic removal from ground water by iron-modified zeolite, J. Chem. Eng. Japan 36 (2003) 1516–1522.

[21] J.L. Cortina, R. Arad-Yellin, N. Miralles, A.M. Sastre, A. Warshawsky, Kinetics studies on heavy metal ions extraction by Amberlite XAD2 impregnated resins containing a bifunctional organophosphorous extractant, React. Funct. Polym. 38 (1998) 269–278.

[22] N.K. Hamadi, X.D. Chen, M.M. Farid, M.G.Q. Lu, Adsorption kinetics for the removal of chromium(VI) from aqueous solution by adsorbents derived from used tyres and sawdust, Chem. Eng. J. 84 (2001) 95–105.

[23] G. Atun, B. Bilgin, A. Kilislioglu, Kinetics of isotopic exchange between strontium polymolybdate and strontium ions in aqueous solution, Appl. Radiat. Isot. 56 (2002) 797–803.

[24] Joint Commission of Powder Diffraction Standards Data Base (JCPDS), Shimadzu, Japan, 1995.

[25] M.J. Kang, B.S. Hahn, Adsorption behavior of aqueous europium on kaolinite under various disposal conditions, Korean J. Chem. Eng. 21 (2004) 419–424.

[26] E. Guibal, C. Milot, J.M. Tobin, Metal-anion sorption by chitosan beads; equilibrium and kinetics studies, Ind. Eng. Chem. Res. 37 (1998) 1454–1468.

[27] Y.S. Ho, G. McKay, A kinetics study of dye sorption by biosorbent waste product pith, Resour. Conserv. Recycl. 25 (1999) 171–193.

[28] R. Qadeer, J. Hanif, I. Hanif, Uptake of thorium ions from aqueous solutions by molecular sieves (13× type) powder, J. Radioanal. Nucl. Chem. 190 (1995) 103–112.
[29] M. Alkan, O. Demirbas, S. Alikcapa, M. Dogan, Sorption of acid red 57 from aqueous solution onto sepiotite, J. Hazard. Mater. B116 (2004) 135–145.
[30] G. McKay, Y.S. Ho, The sorption of lead (II) on peat, Water Res. 33 (1999) 585–587.
[31] G. McKay, Y.S. Ho, Pseudo-second order model for sorption processes, Process Biochem. 34 (1999) 451–460.
[32] W.J. Weber, J.M. Morris, Kinetics of adsorption on carbon from solutions, J. Sanit. Eng. Div. Am. Soc. Eng. 89 (1963) 31–39.
[33] F. Helfferich, Ion Exchange, Mc Graw Hill, New York, 1962.
[34] G.M. Walker, L.R. Weatherly, Kinetics of acid dye adsorption on GAC, Water Res. 33 (1999) 1895–1899.
[35] K.G. Scheckel, D.L. Sparks, Temperature effects on nickel sorption kinetics at mineral–water interface, Soil. Sci. Soc. Am. J. 65 (2001) 719–728.
[36] D. Mohan, K.P. Singh, Single and multi-component adsorption of cadmium and zinc using activated carbon derived from bagasse an agricultural waste, Water Res. 36 (2002) 2304–2318.